



TRUNCATED MODEL TESTS FOR MOORING LINES OF A SEMI-SUBMERSIBLE PLATFORM AND ITS EQUIVALENT COMPENSATED METHOD

Dong-Sheng Qiao

Deepwater Engineering Research Center, Dalian University of Technology, Dalian, P. R. China, qds903@163.com

Jin-Ping Ou

Deepwater Engineering Research Center, Dalian University of Technology, Dalian, P. R. China. State Key Laboratory of Coastal and Offshore Engineering, Dalian University of Technology, Dalian, P. R. China.

Follow this and additional works at: <https://jmstt.ntou.edu.tw/journal>



Part of the [Ocean Engineering Commons](#)

Recommended Citation

Qiao, Dong-Sheng and Ou, Jin-Ping (2014) "TRUNCATED MODEL TESTS FOR MOORING LINES OF A SEMI-SUBMERSIBLE PLATFORM AND ITS EQUIVALENT COMPENSATED METHOD," *Journal of Marine Science and Technology*. Vol. 22: Iss. 2, Article 3.

DOI: 10.6119/JMST-013-0108-1

Available at: <https://jmstt.ntou.edu.tw/journal/vol22/iss2/3>

This Research Article is brought to you for free and open access by Journal of Marine Science and Technology. It has been accepted for inclusion in Journal of Marine Science and Technology by an authorized editor of Journal of Marine Science and Technology.

TRUNCATED MODEL TESTS FOR MOORING LINES OF A SEMI-SUBMERSIBLE PLATFORM AND ITS EQUIVALENT COMPENSATED METHOD

Acknowledgements

This paper was financially funded in part by National Basic Research Program of China (Grant NO. 2011CB013702; 2011CB013703), National Natural Science Foundation of China (Grant NO. 51209037), and China Postdoctoral Science Foundation Funded Project (Grant NO. 2012M510811).

TRUNCATED MODEL TESTS FOR MOORING LINES OF A SEMI-SUBMERSIBLE PLATFORM AND ITS EQUIVALENT COMPENSATED METHOD

Dong-Sheng Qiao¹ and Jin-Ping Ou^{1,2}

Key words: truncated, model test, viscous damper, semi-submersible platform.

ABSTRACT

This study conducted a model test of 1:100 model scale of a semi-submersible platform with a 1500 m full-depth mooring system in the Joint Laboratory of Wind Tunnel & Wave Flume at Harbin Institute of Technology. A truncated mooring system of 400 m water depth was designed based on the static equivalent principle. The semi-submersible platform was tested under regular wave excitation periods that ranged from 10 s to 45 s and one year of irregular wave conditions in the South China Sea. The results validated the feasibility of using numerical simulation in the motions calculation of semi-submersible platform and showed that mooring damping may contribute significantly to the total damping of deepwater floating platform in the low frequency range. The viscous damper was designed to simulate the contribution of mooring damping and added to the numerical simulation of the motion calculation of semi-submersible platform with the truncated mooring line. The numerical simulation results were compared with the motion calculation of semi-submersible platform with the full-depth mooring line. This method can help solve the differences in the dynamics of truncated model tests that are typically used in ocean engineering.

I. INTRODUCTION

Given that the oil industry has been increasingly its efforts and activities on deeper water, suitable floating platforms such as semi-submersible, tension-leg and Spar platforms are

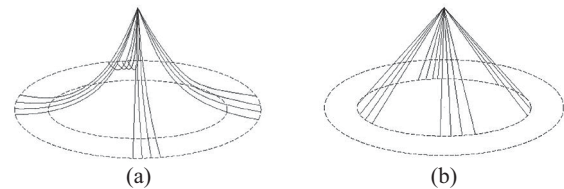


Fig. 1. (a) Catenary mooring system, and (b) Taut mooring system.

becoming more widely applied in practical projects. The main consideration when designing a suitable floating platform is the method by which its motions can be accurately predicted under various complicated loads in the deep sea. Common numerical simulation and physical model test are two approaches that are currently used to predict floating platform motions. The calculation results of a numerical simulation seem refutable and unauthentic because of the number of presumptions or the amount of empirical data introduced into the simulation. Thus, the physical model test can be considered the most precise method in the prediction of floating platforms motions under environmental loads.

Except for the tension-leg platform (TLP), which adopts a tension leg in the vertical direction to moor the upper floating platform, other platforms adopt outspread mooring systems, such as the traditional catenary mooring system and the recently developed taut mooring system, as shown in Fig. 1. During model testing, the catenary and taut mooring systems occupy large spaces, and the intact model tests cannot be completed in the current wave basins by adopting the normal reduced scale that is consistent with the upper platform. Thus, the use of hybrid testing or hybrid verification, which is an experimental technique combining numerical simulation with a truncated physical model test, appears to be the most realistic alternative [11]. Before the experiment, giving the limitation of the wave basin scale, a mooring system is truncated according to standard operating procedure. The truncated mooring system is modeled by using a numerical method and is then operated through a standard reduced scale model that is consistent with the upper platform. Both motions and tensions

Paper submitted 11/18/11; revised 11/08/12; accepted 01/08/13. Author for correspondence: Dong-Sheng Qiao (e-mail: qds903@163.com).

¹ Deepwater Engineering Research Center, Dalian University of Technology, Dalian, P. R. China.

² State Key Laboratory of Coastal and Offshore Engineering, Dalian University of Technology, Dalian, P. R. China.

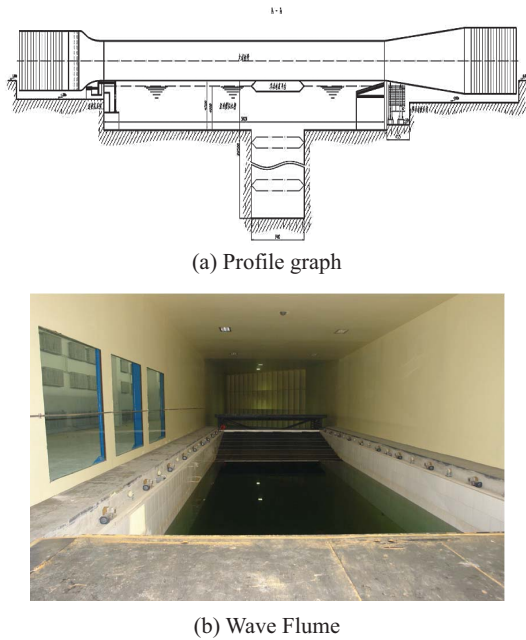


Fig. 2. Image of Joint Laboratory of Wind Tunnel & Wave Flume.

are considered during this procedure. A number of scholars have recently studied truncated mooring systems and achieved significant results [5, 10, 12]. The two key points are the method by which to design the truncated mooring system accurately and that by which to analyze the differences of the dynamic characteristics between a truncated mooring line and its corresponding full-depth mooring line.

Luo *et al.* [8] introduced a method for the preliminary confirmation of the parameters of equivalent truncated mooring systems. Su *et al.* [13] investigated the equivalent design of vertical and horizontal truncated mooring systems and the static equivalent design of a Spar platform mooring system. Chen *et al.* [3] studied the difference between the truncated and corresponding full-depth mooring line model via a model test. Chen *et al.* [2] used three types of numerical calculation software to study the dynamic tension characteristic of a truncated mooring line and its corresponding full-depth mooring line model under different loads.

In this study, the mooring system of a semi-submersible platform with a 1500 m full-depth mooring system was examined. Model tests were conducted in the Joint Laboratory of Wind Tunnel & Wave Flume at the Harbin Institute of Technology. The flume is 50 m long, 5.5 m wide, and has an operating water depth of 4 m, as shown in Fig. 2. A truncated mooring system with a water depth of 400 m was designed according to the dimensions of the flume with a model scale of 1:100. The mooring system primarily offers restoring forces to the platform, such that equivalent static restoring forces were chosen when designing the truncated mooring system. The differences in the motions of the semi-submersible platform and the mooring line tension were then compared using the numerical simulation and model test results.

Table 1. Parameters of semi-submersible platform.

Item	Value	Unit
pontoon	$114.07 \times 20.12 \times 8.54$	m
column	$17.385 \times 17.385 \times 21.46$	m
deck	$74.42 \times 74.42 \times 8.60$	m
bottom derrick	$17 \times 17 \times 42$	m
upper derrick	$17 \times 17 \times 22$	m
water gap	14	m
tonnage	48206.8	t



Fig. 3. Experimental models of the semi-submersible platform.

A new model testing method that differs from the hybrid model testing method was established to determine the motion responses of the floating platform directly. Viscous dampers were designed and directly added to the platform to compensate for the contribution of truncated mooring damping. The viscous damper design parameters were obtained as follows: the contributions of mooring damping to the floating platform were calculated in the truncated mooring line and its corresponding full-depth mooring line model. The differences of the values resulting from the two calculations were then used in designing a viscous damper.

II. EQUIVALENT WATER DEPTH TRUNCATED MODEL TEST DESIGN

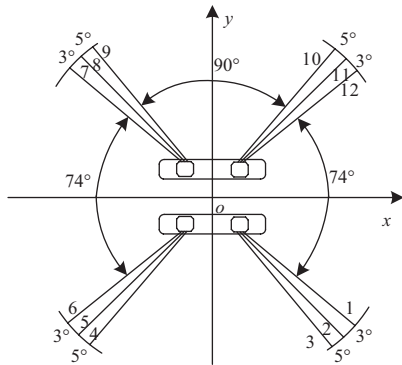
1. Experiment Set-up

The main structure of the semi-submersible platform comprised two pontoons, four columns, a deck and a derrick. The specific parameters are shown in Table 1. The experimental model of the semi-submersible platform following Froude number scaling is shown in Fig. 3.

The semi-submersible platform was oscillated under regular or irregular wave excitation. The experiment was conducted with the semi-submersible platform at selected regular wave excitation in the x axes. Given the capacity of the wave maker in the laboratory, the wave period was changed from 10 s to 45 s, and the wave height was 6 m, which were all given

Table 2. Parameters of the full-depth mooring line.

Item	R4S chain (upper)	Polyester (middle)	R4S Chain (bottom)
Diameter (m)	0.084	0.160	0.084
Length (m)	231	2650	1500
Axial stiffness (t)	63300	8280	63300
Mass in water (kg/m)	138	4.09	138

**Fig. 4. Configuration of the semi-submersible mooring system.**

in the prototype scale. The irregular sea conditions were one year design conditions in the South China Sea. The wave spectrum used was a JONSWAP spectra with significant wave height of 6.0 m and spectral peak period of 11.2 s. The wind velocity at 10 m height was 23.1 m/s. The tensions of a representative mooring line were recorded using a cylindrical tension sensor at the top end of the mooring line. The maximum tension of the cylindrical tension sensor was 50 N with 0.1% precision. Moreover, the sensor can be used under the water. The type of tension sensor was an LA2, which is produced by Midwest Group in China. The motions of the semi-submersible platform were recorded using a ‘CCD-measured sensor’. The sensor is a six component sensor measuring apparatus of floating body with binocular CCD, which was produced by Li *et al.* [6] at Dalian University of Technology.

2. Semi-submersible Platform Mooring System

The full scale semi-submerge platform mooring system with a water depth of 1500 m comprised 12 hybrid mooring lines. A plan view of the line configuration is shown in Fig. 4. The full-depth single mooring line comprised chain-polyester-chain, and the main parameters are listed in Table 2. The initial tension of mooring line was 1200 kN and the distance between the anchor and fairlead was 3999 m.

3. Static Equivalent Design

The maximum operating water depth in the Joint Laboratory of Wind Tunnel & Wave Flume in Harbin Institute of Technology is 4 m. Thus, the full-depth mooring system with a water depth of 1500 m was truncated with a water depth

Table 3. Parameters of truncated mooring line.

Item	Wire (upper)	Elastic material (bottom)
Diameter (m)	0.1	0.2
Length (m)	230.4	120
Axial stiffness (t)	Inelastic	130.5
Mass in water (kg/m)	136	170
Buoy (kN)	500	

Table 4. Parameters of experimental mooring line.

Item	Rope (upper)	Spring (bottom)
Diameter (m)	0.001	0.002
Length (m)	2.304	1.20
Axial stiffness (t)	Inelastic	0.1305
Mass in water (kg/m)	0.0133	0.0166
Buoy (N)	0.488	

of 400 m in a model scale of 1:100. In practice, the design of the truncated mooring system based on the static equivalent principle may be guided by the following rules:

- (1) Model the correct representative single mooring line tension-horizontal displacement characteristics;
- (2) Model the correct mooring system total horizontal force-horizontal displacement and total vertical force-horizontal displacement characteristic in the x direction;
- (3) Model the correct mooring system total vertical force-vertical displacement characteristic;
- (4) Model the correct quasi-static coupling between the semi-submersible platform’s surge and pitch responses.

Considering the gravity, tension, current force, and mooring line extension, the piecewise extrapolation method can be used for the static analysis of a multi-component mooring line [9]. The parameters of a truncated mooring line are listed in Table 3, and the parameters of its corresponding experimental mooring line are listed in Table 4. The buoy was positioned on the connection between the two mooring line segments. The shapes of the truncated and full-depth mooring lines are plotted in Fig. 5, and the experimental model of the truncated mooring line is shown in Fig. 6. Current velocity was ignored in the design of the truncated mooring line.

III. GOVERNING EQUATIONS AND FORMULATION

1. Governing Equation of Mooring Line

During the motion response analysis, the mooring line was generally assumed to be a completely flexible component and the motion governing equation proposed by Berteaux [1] was used.

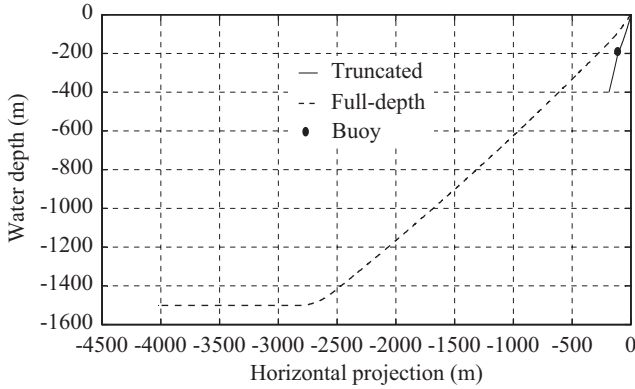


Fig. 5. Shapes of truncated and full-depth mooring line.

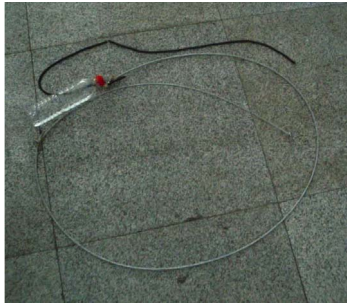


Fig. 6. Experimental models of the truncated mooring line.

$$(m + m_a) \left(\frac{\partial \vec{V}}{\partial t} - \frac{\partial \vec{U}}{\partial t} \right) = \vec{F}_{Dn} + \vec{F}_{Dt} + \vec{F}_{In} + \vec{F}_{It} + \vec{T} + \vec{G} \quad (1)$$

$$\vec{F}_{Dn} = \frac{1}{2} \rho_w C_{Dn} D \Delta \vec{V}_n \left| \Delta \vec{V}_n \cdot \Delta \vec{V}_n \right|^{1/2} \quad (2)$$

$$\vec{F}_{Dt} = \frac{1}{2} \rho_w C_{Dt} \pi D \Delta \vec{V}_t \left| \Delta \vec{V}_t \right| \quad (3)$$

$$\vec{F}_{In} = \frac{1}{4} \rho_w \pi D^2 C_{In} \left(\frac{\partial \vec{V}}{\partial t} - \frac{\partial \vec{U}}{\partial t} \right) \quad (4)$$

$$\vec{F}_{It} = \frac{1}{4} \rho_w \pi D^2 C_{It} \left(\frac{\partial \vec{V}}{\partial t} - \frac{\partial \vec{U}}{\partial t} \right) \quad (5)$$

where m is the mass of mooring line, m_a is the added mass of mooring line, \vec{V} is the velocity vector of the mooring line, \vec{U} is the velocity vector of fluid, \vec{F}_{Dn} is the mooring line normal drag forces (per unit length), \vec{F}_{Dt} is the mooring line tangential drag forces (per unit length), \vec{F}_{In} is the mooring line normal inertia forces (per unit length), \vec{F}_{It} is the mooring line

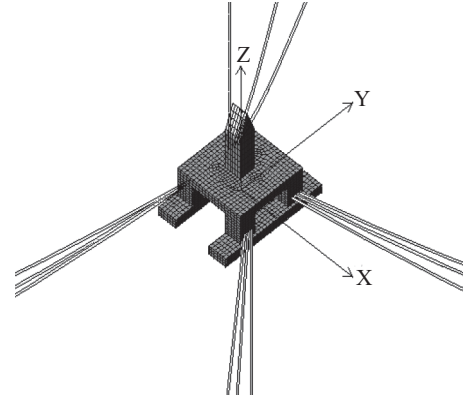


Fig. 7. Coupled analysis model.

tangential inertia forces (per unit length), \vec{T} is the tension of mooring line and \vec{G} is the net weight of mooring line, $\rho_w = 1025 \text{ kg/m}^3$ is the fluid density, $C_{Dt} = 0.05$ is the tangential drag coefficient, D is the wire diameter, $\Delta \vec{V}_t$ is the relative tangential velocity of the fluid, $C_{Dn} = 1.2$ is the normal drag coefficient, $\Delta \vec{V}_n$ is the relative normal velocity of the fluid. $C_{In} = 0.25$ is the tangential inertial coefficient and $C_{In} = 0.5$ is the normal inertial coefficient. $\left(\frac{\partial \vec{V}}{\partial t} - \frac{\partial \vec{U}}{\partial t} \right)$ is the relative acceleration between fluid and mooring line.

As far as formula (1) is concerned, the motion governing equation is a strong complex time-varying non-linear equation which is solved using a numerical method. The non-linear finite element method was used for the solution in this paper. In ABAQUS, the mooring line is simulated as a hybrid beam element [15] and the Newton-Raphson iterative method was used to solve the non-linear problem directly.

To calculate the coupled motion, the commercially available program AQWA was employed. The wave forces on the semi-submersible platform were calculated based on diffraction theory by the boundary element method. The coupled analysis model is shown in Fig. 7.

In AQWA, the platform structure is treated as a rigid body, and the wind loads and wave forces acting on the platform are described as below.

2. Wave Forces Calculation

In the numerical simulation, the transient wave forces acting on the platform under irregular waves are approximately given as follows [4, 16]:

$$F_i(t) = F_i^{(1)}(t) + F_i^{(2)}(t) \quad (i = 1, 2, \dots, 6) \quad (6)$$

where $F_i^{(1)}(t)$ and $F_i^{(2)}(t)$ are the first and second order wave forces. They are given as:

$$F_i^{(1)}(t) = \int_0^t h_i^1(t-\tau)\eta(\tau)d\tau \quad (i=1, 2, \dots, 6) \quad (7)$$

$$m_{kj} = a_{kj}(\infty) \quad (13)$$

$$F_i^{(2)}(t) = \int_0^t \int_0^t h_i^2(t-\tau_1, t-\tau_2)\eta(\tau_1)\eta(\tau_2)d\tau_1d\tau_2 \quad (i=1, 2, \dots, 6) \quad (8)$$

$$K_{kj}(t) = \frac{2}{\pi} \int_0^\infty b_{kj}(\omega)\cos(\omega t)d\omega \quad (14)$$

where $h_i^1(t)$ and $h_i^2(t)$ are the first and second order impulse response functions in the time domain, and $\eta(t)$ is the sea surface elevation. $h_i^1(t)$ and $h_i^2(t)$ are given as:

where a_{kj} and b_{kj} are, respectively, the added mass and damping of the platform in frequent domain. Eq. (12) can be described as:

$$h_i^1(t) = \text{Re} \left\{ \frac{1}{\pi} \int_0^\infty H_i^{(1)}(\omega)e^{i\omega t}d\omega \right\} \quad (9)$$

$$\ddot{\xi} = F[t, \xi, \dot{\xi}] = \frac{1}{M_{kj} + m_{kj}} [F_j(t) + G_j(t) - \int_{-\infty}^t \dot{\xi}_j(\tau)K_{kj}(t-\tau)d\tau - B_k\dot{\xi}(t) - C_{kj}\xi_j(t)] \quad (15)$$

$$h_i^2(t_1, t_2) = \text{Re} \left\{ \frac{1}{2\pi^2} \int_0^\infty \int_0^\infty H_i^{(2)}(\omega_1, \omega_2)e^{i(\omega_1 t_1 + \omega_2 t_2)}d\omega_1d\omega_2 \right\} \quad (10)$$

where $H_i^1(\omega)$ and $H_i^2(\omega_1, \omega_2)$ are the first and second square order transfer functions for wave force [14].

Eq. (15) is solved by *Runge-Kutta* method in this paper. The displacement and velocity of the platform at the time step $t + \Delta t$ are written as:

3. Wind Forces Calculation

The wind loads acting on the platform are given as:

$$F_{wind,H} = \frac{1}{2} C_{d,H} \rho A_H V_H^2 \quad (11)$$

where V_H is the average wind velocity at the height H above sea level, $\rho = 1.29 \text{ kg/m}^3$ is the density of air, A_H is the projected area of platform in the direction of wind. $C_{d,H}$ is the wind pressure coefficient, obtained from wind tunnel experiment with a 1:150 scaled model [17].

4. Governing Equations and Formulation of Semi-submersible Platform

The equation of motion for the coupled system in the time domain is given as follows:

$$(M_{kj} + m_{kj})\ddot{\xi}_j(t) + \int_{-\infty}^t \dot{\xi}_j(\tau)K_{kj}(t-\tau)d\tau + B_k\dot{\xi}_j(t) + C_{kj}\xi_j(t) = F_j(t) + G_j(t) \quad (j=1, 2, \dots, 6) \quad (12)$$

where M_{kj} is the mass matrices of the platform, C_{kj} is the hydrostatic restoring stiffness, B_k is the viscous damping of the system, $G_j(t)$ is the mooring force, $F_j(t)$ is the external forces which contain wind loads and wave forces. Assuming the platform motion is related to simple harmonic motion and compared with the motion equation of the platform in frequent domain, any motion of the platform can be described by Eq. (12) [7]. M_{kj} and $K_{kj}(t)$ are given as:

$$\xi(t + \Delta t) = \xi(t) + \Delta t \dot{\xi}(t) + \Delta t(M_1 + M_2 + M_3)/6 \quad (16)$$

$$\dot{\xi}(t + \Delta t) = \dot{\xi}(t) + (M_1 + 2M_2 + 2M_3 + M_4)/6 \quad (17)$$

where Δt is taken as the time step, and

$$M_1 = \Delta t F[t, \xi(t), \dot{\xi}(t)],$$

$$M_2 = \Delta t F[t + \frac{\Delta t}{2}, \xi(t) + \frac{\Delta t \dot{\xi}(t)}{2}, \dot{\xi}(t) + \frac{M_1}{2}],$$

$$M_3 = \Delta t F[t + \frac{\Delta t}{2}, \xi(t) + \frac{\Delta t \dot{\xi}(t)}{2} + \frac{\Delta t M_1}{2}, \dot{\xi}(t) + \frac{M_2}{2}],$$

$$M_4 = \Delta t F[t + \frac{\Delta t}{2}, \xi(t) + \Delta t \dot{\xi}(t) + \frac{\Delta t M_2}{2}, \dot{\xi}(t) + M_3].$$

Function $F[\Delta t, \xi, \dot{\xi}]$ can be solved using the displacement $\xi(t)$ and velocity $\dot{\xi}(t)$ of the platform at the time t , and the displacement $\xi(t + \Delta t)$ and velocity $\dot{\xi}(t + \Delta t)$ of the platform at the time step $t + \Delta t$ can be calculated by using Eqs. (16) and (17). The process will be repeated until the computation is completed.

5. Calculating Mooring Damping Forces

The energy dissipated E during one surge oscillation of period τ is given by:

$$E = \int_0^\tau T_n \frac{dq_n}{dt} dt \quad (18)$$

where T_n is the component of tension in the direction n and q_n is the instantaneous displacement in that direction.

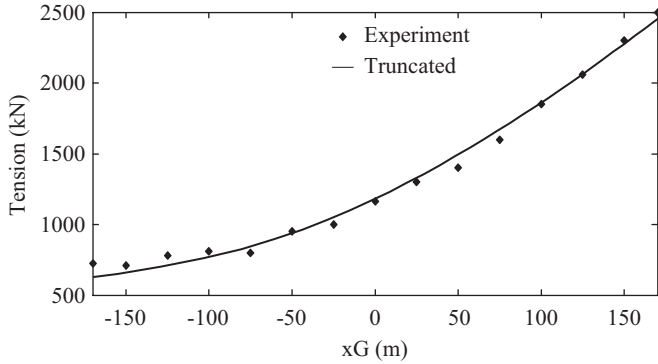


Fig. 8. Tension-horizontal displacement characteristic curve.

Expressing this damping in terms of an equivalent linear damping coefficient B_n is often convenient. The instantaneous value of T_n can then be approximately given by:

$$T_n = B_n \frac{dq_n}{dt} \quad (19)$$

If the oscillation is sinusoidal with an amplitude, q_0 , and a period, τ , the approximate absorbed energy E is given by:

$$E = \int_0^\tau T_n \frac{dq_n}{dt} dt = B_n \int_0^\tau \left[\frac{dq_n}{dt} \right]^2 dt = \frac{2\pi^2 q_0^2 B_n}{\tau} \quad (20)$$

Consequently, the energy dissipated by the mooring line during one surge oscillation can be computed, and the linear damping coefficient is then obtained by:

$$B_n = \frac{E\tau}{2\pi^2 q_0^2} \quad (21)$$

The dissipated energy E can be obtained by integrating the work done with the upper tension during one surge oscillation, which requires the use of a finite element dynamics program.

IV. ANALYSIS OF MODEL TEST RESULTS

1. Static Verification

The static stiffness of the mooring line in the x direction needs to be verified specifically at the equilibrium, average, and maximum positions because of the maximum effect of a platform's surge motion on mooring line tension. In the static tests, the platform was moved slowly to a selected position in the x direction, and the mooring line tension was recorded after the motion of the mooring line completely stopped. The static test results are plotted in Fig. 8, showing excellent agreement between the measurements and the numerical simulation results.

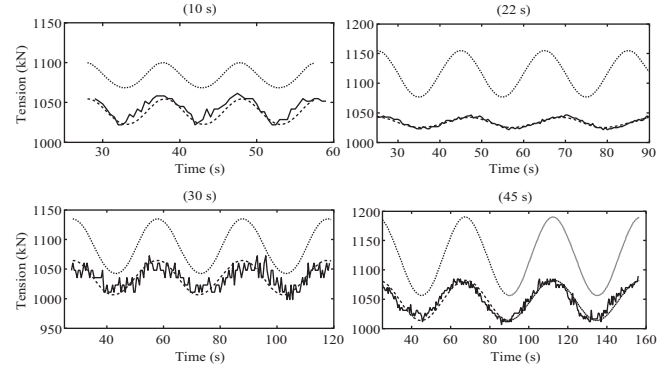


Fig. 9. Tension time series (10 s, 22 s, 30 s, and 45 s; Dotted line: Full-depth; Solid line: Experiment; Dashed line: Truncated).

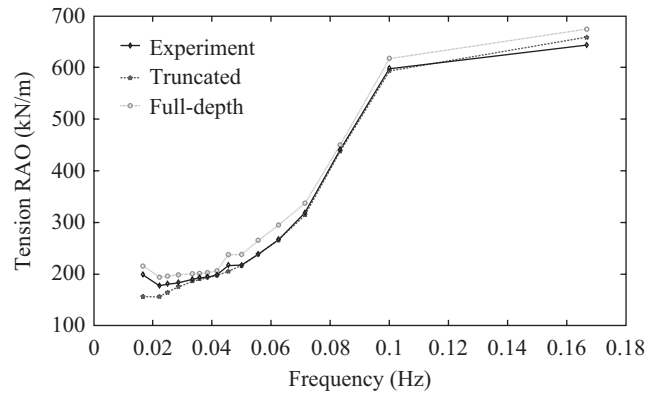


Fig. 10. RAO of mooring line tension.

2. Regular Wave Excitation Tests

The tension time series of the full-depth and truncated mooring lines were obtained based on the numerical simulation. The tension time series of the full-depth, truncated, and experimental mooring lines when the platform was experimented at selected regular wave excitations are shown in Fig. 9. The response amplitude ratios (RAO) of the line tension to fairlead motion are shown in Fig. 10. RAO is defined as the average of peak-to-peak line tension divided by the average peak-to-peak fairlead motion.

As shown in Fig. 9, the tension time series of the truncated and experimental mooring lines are in excellent agreement and have the same period as the wave excitation period. The results show that the numerical simulation is credible. The tensions of the full-depth mooring line are approximately 15% greater than those of the truncated and experimental mooring lines, thus indicating that the truncated mooring line is subjected to less tension than the full-depth mooring line. As shown in Fig. 10, the numerical simulation results show better agreement with the experiment results in the low-frequency range (frequency < 0.07 Hz), but some disagreement with the experimental results in the wave-frequency range (frequency > 0.07 Hz). The RAO of full-depth mooring line

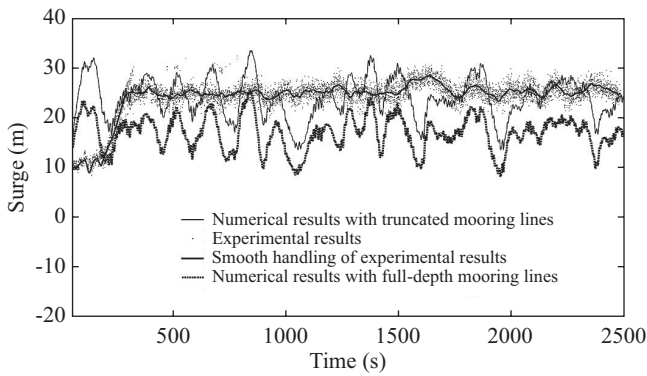


Fig. 11. Time series of surge motion.

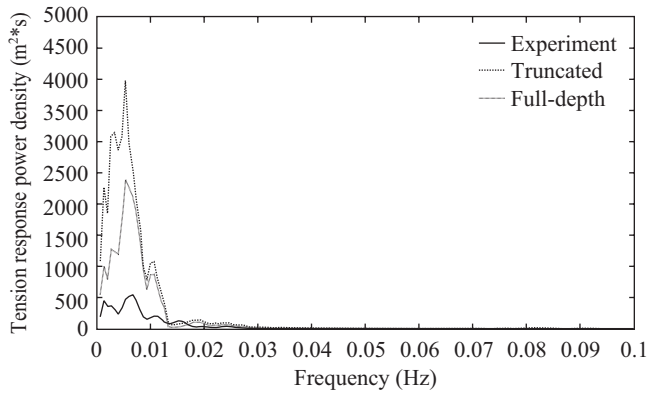


Fig. 12. Surge motion spectra.

tension is greater than those of the truncated and experimental mooring lines.

3. Irregular Wave Excitation Tests

The surge motion time series of the semi-submersible platform with full-depth, truncated, and experimental mooring lines when the platform was experimented at irregular wave excitation are shown in Fig. 11. By using Fast Fourier Transform (FFT), the surge motion spectra of the platform are plotted in Fig. 12. Based on Fig. 11, the results show that the surge motion of the semi-submersible platform with full-depth mooring lines is smaller than that with truncated mooring lines, and the average surge motion of experimental results is in agreement with the corresponding prediction of numerical simulation using truncated mooring lines. The shapes of the three spectra are similar, whereas their peak values differ.

The tension time series of the full-depth, truncated, and experimental mooring lines when the platform was experimented at irregular wave excitation are shown in Figs. 13 and 14. By using FFT, the top-tension spectra of the mooring lines are plotted in Fig. 15. As shown in Figs. 13 to 15, the results indicate that the truncated mooring line is subjected to less tension than the full-depth mooring line, although the shapes of the two spectra are similar. The peak of truncated mooring line is smaller than that of the full-depth mooring

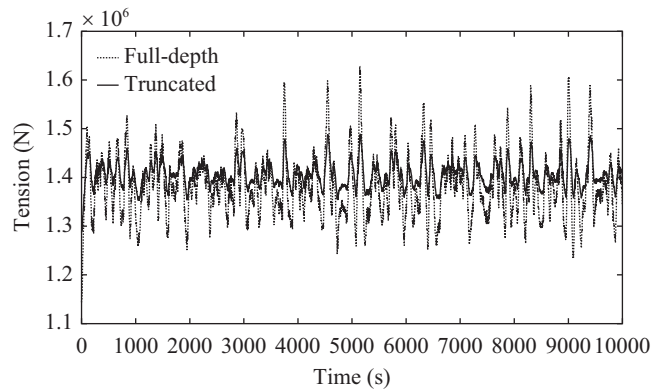


Fig. 13. Tension time series of truncated and full-depth mooring lines.

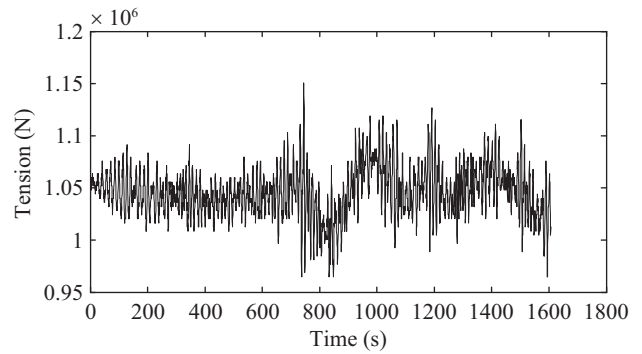


Fig. 14. Tension time series of the experimental mooring line.

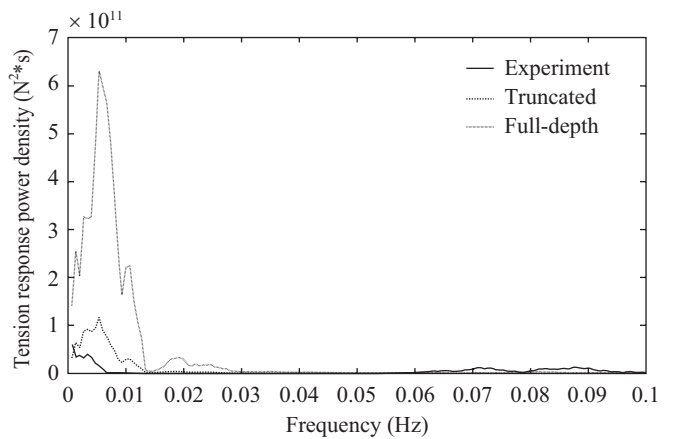


Fig. 15. Mooring line top-tension spectra.

line. The tension of the experimental mooring line is slightly less than that of the truncated mooring line, and their top-tension spectra are like-wise similar.

As shown in Figs. 11 to 15, the experimental results validate the availability of numerical simulation in the mooring line tension calculation and motion calculation of the semi-submersible platform. The truncated mooring lines provide less mooring damping contribution to the total damping of

Table 5. Calculation parameters variation and results.

Case	Excitation (m)	Mooring damping (kNs/m)						Mean	Error (%)
		Full-depth		Truncated		Value difference			
		B_x	B_z	B_x	B_z	B_x	B_z		
1.1	$X = 4 \sin(\frac{2\pi}{30}t)$	40.1	none	10.0	none	30.1	none	$B_x = 30.8$	2.4
1.2	$X = 6 \sin(\frac{2\pi}{30}t)$	45.1		17.2		28.0			10.1
1.3	$X = 8 \sin(\frac{2\pi}{30}t)$	49.7		22.4		27.2			12.8
1.4	$X = 10 \sin(\frac{2\pi}{30}t)$	53.4		25.1		28.0			8.8
1.5	$X = 12 \sin(\frac{2\pi}{30}t)$	56.4		27.1		29.5			5.0
1.6	$X = 13.9 \sin(\frac{2\pi}{30}t)$	58.9		29.5		29.5			4.6
1.7	$X = 10 \sin(\frac{2\pi}{15}t)$	58.5		24.6		33.9			9.3
1.8	$X = 10 \sin(\frac{2\pi}{20}t)$	55.3		23.2		32.1			3.9
1.9	$X = 10 \sin(\frac{2\pi}{25}t)$	53.6		24.1		29.5			4.4
1.10	$X = 10 \sin(\frac{2\pi}{40}t)$	54.6		26.2		28.4			8.4
1.11	$X = 10 \sin(\frac{2\pi}{50}t)$	57.1		28.0		29.1			5.8
1.12	$X = 10 \sin(\frac{2\pi}{70}t)$	64.0		32.6		31.4			1.8
1.13	$X = 10 \sin(\frac{2\pi}{90}t)$	71.9		36.0		36.0			14.4
1.14	$X = 10 \sin(\frac{2\pi}{130}t)$	85.5		51.3		34.2			9.9
1.15	$X = 10 \sin(\frac{2\pi}{180}t)$	99.8		64.9		34.9			11.8
1.16	$X = 10 \sin(\frac{2\pi}{250}t)$	110.0		77.0		33.0			6.7
2.1	$Z = 0.4 \sin(\frac{2\pi}{1.8}t)$	none	17.1	none	2.7	none	14.4	$B_z = 16.0$	11.4
2.2	$Z = 0.6 \sin(\frac{2\pi}{1.8}t)$		20.2		4.0		16.2		1.0
2.3	$Z = 0.8 \sin(\frac{2\pi}{1.8}t)$		28.5		11.4		17.1		6.4
2.4	$Z = 1.0 \sin(\frac{2\pi}{1.8}t)$		42.1		25.3		16.8		5.0
2.5	$Z = 1.2 \sin(\frac{2\pi}{1.8}t)$		47.7		29.6		18.1		11.7
2.6	$Z = 1.5 \sin(\frac{2\pi}{1.8}t)$		54.8		36.2		18.6		14.1
2.7	$Z = 1.0 \sin(\frac{2\pi}{1.4}t)$		26.7		10.7		16.0		0.1
2.8	$Z = 0.4 \sin(\frac{2\pi}{2.0}t)$		21.7		7.6		14.1		13.4
2.9	$Z = 0.4 \sin(\frac{2\pi}{2.3}t)$		28		12.6		15.4		3.9
2.10	$Z = 0.4 \sin(\frac{2\pi}{2.5}t)$		29.7		14.1		15.6		2.6

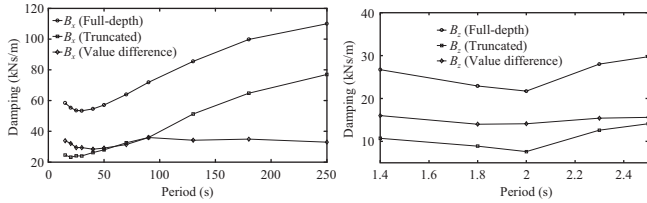


Fig. 16. Effect of the excitation period in the x and z directions.

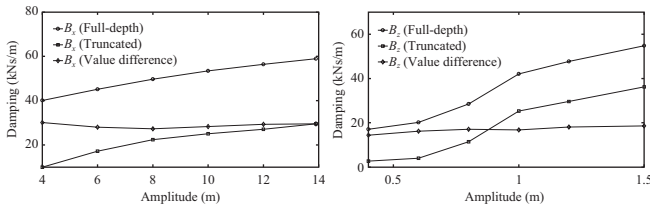


Fig. 17. Effects of the excitation amplitude in the x and z directions.

the deepwater floating platform because of the differences of the dynamics between the truncated and full-depth mooring lines. This inferior mooring damping capability of truncated mooring lines needs to be solved by using other approaches.

V. EQUIVALENT COMPENSATION METHOD USING VISCOUS DAMPER

1. Calculation of the Parameters of Viscous Damper Design

As shown in Fig. 12, the surge response of the semi-submersible platform is mainly in the low-frequency range. The experimental results for the heave motion of the semi-submersible platform is not ideal with those of numerical simulation because of the width limitation of the Joint Laboratory of Wind Tunnel & Wave Flume at the Harbin Institute of Technology. The numerical simulation method has been validated via the surge motion. Thus, the numerical simulation results for the heave motion of the semi-submersible platform can be used in the succeeding calculations. Consequently, the excitations of the mooring line top end are listed in Table 5 (APPENDIXES).

According to the calculation method for mooring damping above and the excitations of the mooring line top end, mooring damping has two components in the x and z axes, denoted by B_x and B_z , respectively. The effects of mooring line top end excitation period and amplitude on mooring damping are shown in Figs. 16 and 17, respectively. As the excitation period increases, damping B_x increases, but damping B_z shows only a minimal change. As the excitation amplitude increases, damping B_x and damping B_z both increase.

As shown in Figs. 16 and 17, the mooring line top end excitation period and amplitude have similar effects on the mooring damping of full-depth and truncated mooring lines. The value differences of mooring damping between the full-depth and truncated mooring lines are basically constant,

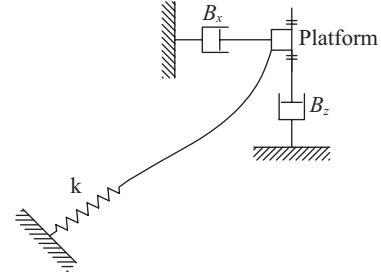


Fig. 18. Configuration of the viscous damper compensated system.

and the value differences of B_x and B_z are likewise constant. The mean value difference between B_x and B_z can be obtained with less than 15% error. Consequently, compared with the semi-submersible platform with full-depth mooring lines, the mean value difference of B_x and B_z can be recognized as the mooring damping contribution of the semi-submersible platform with truncated mooring lines. The mean value difference can be added to B_k in the Eq. (12) for the numerical simulation of the motion calculation of the semi-submersible platform with the truncated mooring lines, thus providing parameters for the design of the viscous damper. The detailed design and manufacture of the viscous damper will be published by the author in the future. The configuration of the viscous damper compensated system used in the model test is shown in Fig. 18.

2. Motion Responses of Semi-submersible Platform

Numerical simulations of the model tests for a 3 h duration under the same irregular sea conditions were performed in three cases by using the previously mentioned calculation method for the semi-submersible platform. The three cases were semi-submersible platforms with full-depth mooring lines, truncated mooring lines, and a viscous damper compensated system in the platform. The statistics of the three simulated surge and heave motions in the time domain are shown in Table 6 (APPENDIXES). The time series and spectra of the three surge and heave motions are plotted in Figs. 19 to 22.

Based on the results of the surge motion of the semi-submersible platform, the average surge motion using the viscous damper compensated system is slightly larger than that using full-depth mooring lines, and both values are less than that using truncated mooring lines. In the low frequency (LF) range, the standard deviations (σ) of surge motion using viscous damper compensated system is less than that using truncated mooring lines. Consistent with the standard deviations, the simulated maximum and minimum offsets in the LF range are also less than that using truncated mooring lines. The decrease in the LF range can be attributed to the fact that the viscous damper compensated system increases the mooring damping contribution of the platform. In the wave frequency (WF) range, the standard deviations (σ) of surge motion show insignificant changes in these cases because when

Table 6. Statistics of motions of semi-submersible platform.

Motion	Surge (m)			Heave (m)		
	Full-depth	Truncated	Viscous damper compensated	Full-depth	Truncated	Viscous damper compensated
Average	16.68	23.69	17.25	-0.83	-0.65	-0.64
σ	3.92	4.64	2.44	0.38	0.38	0.38
Max.	30.59	38.86	25.56	0.62	0.81	0.76
Min.	6.84	13.50	10.65	-2.13	-1.94	-1.92
LF σ	4.18	4.86	2.57	0.05	0.05	0.05
LF Max.	33.05	40.66	25.99	-0.65	-0.44	-0.48
LF Min.	6.69	13.57	11.28	-1.03	-0.83	-0.83
WF σ	1.05	1.03	0.86	0.42	0.42	0.42
WF Max.	4.80	4.93	3.31	1.64	1.64	1.58
WF Min.	-4.21	-4.09	-2.84	-1.43	-1.50	-1.42

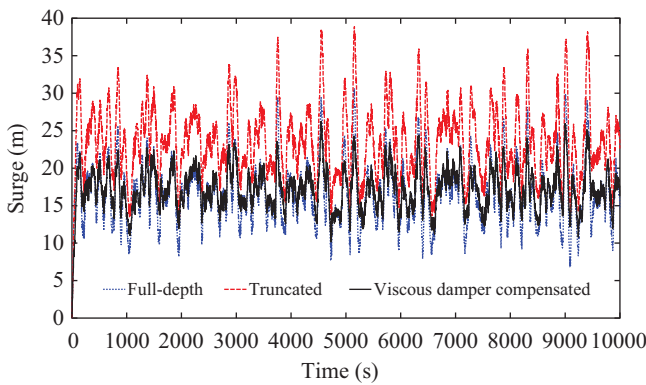


Fig. 19. Time series of surge motions.

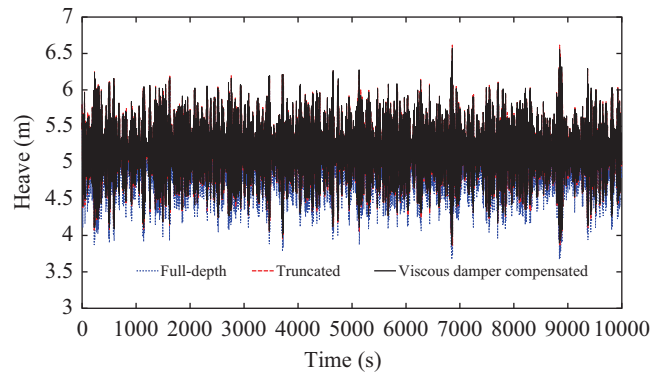


Fig. 21. Time series of heave motions.

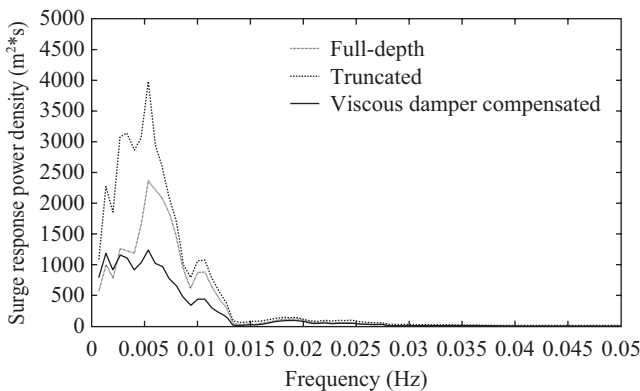


Fig. 20. Surge motions spectra.

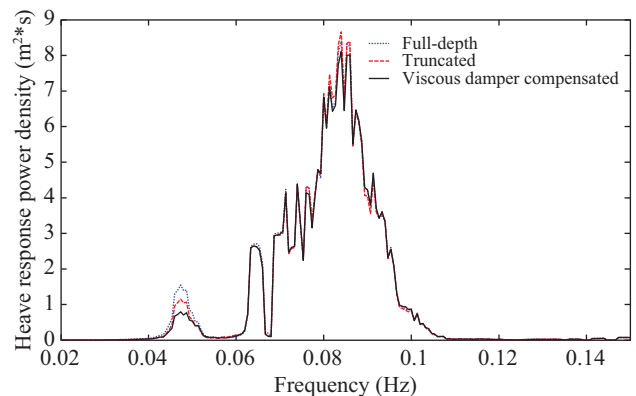


Fig. 22. Heave motions spectra.

the natural frequencies of the semi-submersible platform are far less than the WF range, the inertia forces in the WF range are dominant. Thus, the damping of the mooring lines does not make significant contributions to the reduction of the surge in the WF range. Furthermore, the total mooring line tensions applied on the semi-submersible platform are significantly less than the wave forces on the semi-submersible platform in the WF range.

Based on the results of the heave motion of semi-

submersible platform, the average and standard deviations (σ) of heave motion using viscous damper compensated system in the platform show insignificant changes in these cases because the contribution of mooring damping to the total damping of semi-submersible platform in the heave direction is negligible.

3. Mooring Line Tension

The statistics of the three simulated mooring line tensions in the time domain are given in Table 7. The three tension time

Table 7. Statistics of mooring line tensions (kN).

Tension	Full-depth	Truncated	Viscous damper compensated
Average	1367.4	1401.6	1381.5
σ	62.0	24.8	49.0
Max.	1608.8	1483.0	1569.6
Min.	1219.8	1347.8	1239.3
LF σ	62.2	24.9	47.7
LF Max.	1601.0	1481.0	1565.2
LF Min.	1223.5	1351.1	1257.2
WF σ	7.0	2.3	4.9
WF Max.	63.9	38.4	45.4
WF Min.	-24.9	-8.6	-32.3

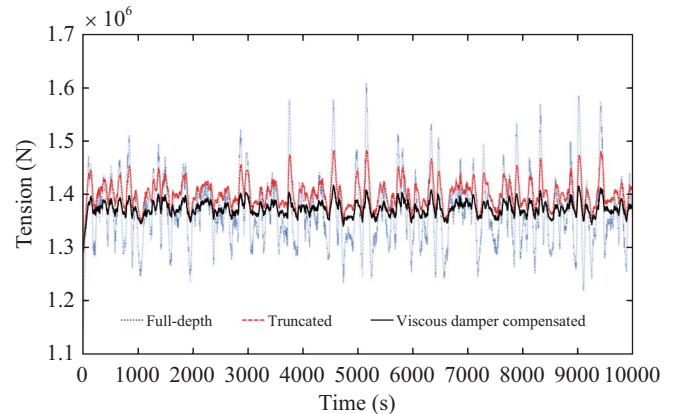
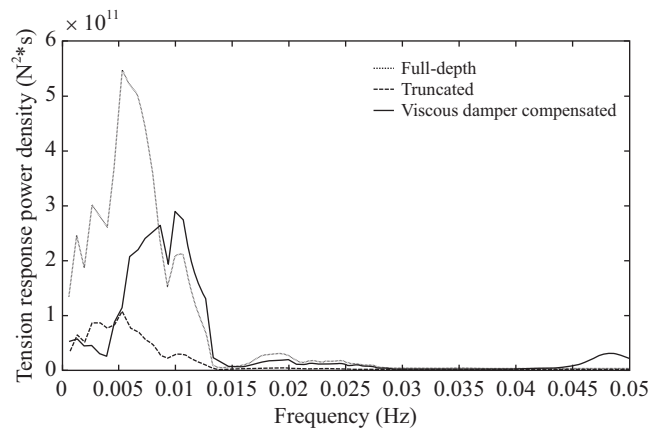
series and their spectra are plotted in Figs. 23 to 24.

The shapes of the surge motions, the mooring line tension spectra, and the dominant frequencies are similar, but their peaks are different. Using the viscous damper compensated system directly in the semi-submersible platform, the truncated mooring line tension is more similar to the full-depth mooring line tension.

VI. CONCLUSION

The results of the tests on mooring line tension and surge motion were compared with those of the numerical simulation via a model test of the semi-submersible platform with a static equivalent truncated mooring system in the Joint Laboratory of Wind Tunnel & Wave Flume at Harbin Institute of Technology. The mooring line tensions and motions of semi-submersible platforms with full-depth mooring lines, truncated mooring lines, and truncated platform with a viscous damper compensation system were compared via numerical simulation, and the preliminary findings are as follows:

- (1) Under regular wave excitation, the tension time series of the truncated and experimental mooring lines are in excellent agreement, but the tensions of the full-depth mooring line are approximately 15% greater than that of the truncated mooring line.
- (2) Under irregular wave excitation, the truncated mooring line is subjected to significantly less tension than the full-depth mooring line, but the shapes of their spectra are similar. The surge motion of the semi-submersible platform with full-depth mooring lines is smaller than that with truncated mooring lines.
- (3) The experimental results validate the feasibility of using numerical simulation for the mooring line tension calculation and motion calculation of semi-submersible platforms. The truncated mooring lines have insignificant mooring damping contribution to the total damping of the deepwater floating platform because of the differences

**Fig. 23. Time series of mooring line tensions.****Fig. 24. Mooring line tension spectra.**

of the dynamics between the truncated and full-depth mooring lines.

- (4) The average surge motion of viscous damper compensated system is slightly greater than that of the full-depth mooring line system, but smaller than that of the truncated mooring line system. In the low-frequency range, the simulated maximum and minimum offsets and the standard deviation of surge motion of the viscous damper compensated system decrease compared with the truncated mooring line system. In the wide-frequency range, the standard deviations of surge motion show insignificant changes in these cases.
- (5) The average and standard deviations of heave motions using the viscous damper compensated system in the platform show insignificant changes in these cases.
- (6) Using the viscous damper compensated system directly in the semi-submersible platform, the truncated mooring line tension becomes more similar to the full-depth mooring line tension.

Consequently, the viscous damper compensated system in the platform with truncated mooring lines can be recognized

as an effective method to solve the differences of the dynamics between truncated and full-depth mooring lines in the model tests.

ACKNOWLEDGMENTS

This paper was financially funded in part by National Basic Research Program of China (Grant NO. 2011CB013702; 2011CB013703), National Natural Science Foundation of China (Grant NO. 51209037), and China Postdoctoral Science Foundation Funded Project (Grant NO. 2012M510811).

REFERENCES

- Berteaux, H. O., *Buoy Engineering*, Wiley Interscience Publication, New York, pp. 170-174 (1976).
- Chen, X. H. and Zhang, J., "Dynamic analysis of mooring lines by using three different methods," *Proceeding of the Eleventh International Offshore and Polar Engineering Conference, Stavanger, Norway*, pp. 635-642 (2001).
- Chen, X. H., Zhang, J., Johnson, P., and Irani, M., "Studies on the dynamics of truncated mooring line," *Proceeding of the Tenth International Offshore and Polar Engineering Conference, Washington, WA, USA*, pp. 94-101 (2000).
- Cummins, W. E., *The Impulse Response Function and Ship Motions*, Technical Report 1661, David Taylor Model Basin, Washington D.C., USA (1962).
- Hong, S., Kim, J. H., Hong, S. W., Jalihal, P., and Ravindran, M., "A hybrid model test of a deepwater OTEC mooring system," *Proceeding of the Fourteenth International Offshore and Polar Engineering Conference, Toulon, France*, pp. 183-188 (2004).
- Li, M. G., Han, B., Zhang, Q., and Wang, J., "A six component measuring apparatus for floating body," *China Offshore Platform*, Vol. 18, No. 3, pp. 35-46 (2003).
- Li, Y. C. and Teng, B., *Wave Action on Maritime Structures*, Second Edition, Ocean Press, Beijing, pp. 90-95 (2002).
- Luo, Y. and Baudic, S., "Predicting FPSO responses using model tests and numerical analysis," *Proceeding of the Thirteenth International Offshore and Polar Engineering Conference, Hawaii, USA*, pp. 167-174 (2003).
- Qiao, D. S. and Ou, J. P., "Static analysis of a deepwater catenary mooring system," *Ship & Ocean Engineering*, Vol. 38, No. 2, pp. 120-124 (2009).
- Rolf, B. and Fabio, G. P., "Hybrid verification of a DICAS moored FPSO," *Proceeding of the Fourteenth International Offshore and Polar Engineering Conference, Toulon, France*, pp. 307-314 (2004).
- Stansberg, C. T., Ormberg, H., and Oritsland, O., "Challenges in deep water experiments: hybrid approach," *Journal of Offshore Mechanics and Arctic Engineering*, Vol. 124, No. 2, pp. 90-96 (2002).
- Stansberg, C. T., Yttervik, R., Oritsland, O., and Kleiven, G., "Hydrodynamic model test verification of a floating platform system in 3000m water depth," *Proceeding of the Nineteenth International Conference of Offshore Mechanics and Arctic Engineering, New Orleans, LA, Paper No. OMAE00-4145* (2000).
- Su, Y. H., Yang, J. M., and Xiao, L. F., "Research on equivalent design method of deepwater mooring system truncated vertically and horizontally," *Ship Building of China*, Vol. 47, Special, pp. 286-292 (2006).
- Teng, B., Li, Y. C., and Dong, G. H., "Second-order wave force on bodies in bi-chromatic waves," *Acta Oceanologica Sinica*, Vol. 21, No. 2, pp. 115-123 (1999).
- Timoshenko, S. P., *Strength of Materials, Part III, Advanced Theory and Problems*, Third Edition, D. Van Nostrand Company, Princeton, New Jersey, pp. 167-168 (1956).
- Van Oortmerssen, G., *The Motions of a Moored Ship in Waves*, Netherlands Ship Model Basin, Publication No. 510, Wageningen, The Netherlands (1976).
- Zhu, H., Ma, Z., Zhai, G. J., Xie, B., Fu, Y. J., and Ou, J. P., "Numerical simulation and wind tunnel tests of wind loads acting on HYSY-981 semi-submersible platform," *Ship & Ocean Engineering*, Vol. 38, No. 5, pp. 149-152 (2009).